Neuroscience 169 (2010) 39–51

M_1-LIKE MUSCARINIC ACETYLCHOLINE RECEPTORS REGULATE FAST-SPIKING INTERNEURON EXCITABILITY IN RAT DENTATE GYRUS

P. H. CHIANG,[a1] W. C. YEH,[a1] C. T. LEE,[a] J. Y. WENG,[a] Y. Y. HUANG[b] AND C. C. LIEN[a]*

[a]*Institute of Neuroscience and Brain Research Center, National Yang-Ming University, 155, Section 2, Li-Nong Street, Taipei, Taiwan*

[b]*Department of Anesthesiology, Cheng Hsin General Hospital, 45, Cheng Hsin Street, Taipei, Taiwan*

Abstract—Cholinergic transmission through muscarinic acetylcholine receptors (mAChRs) plays a key role in cortical oscillations. Although fast-spiking (FS), parvalbumin-expressing basket cells (BCs) are proposed to be the cellular substrates of gamma oscillations, previous studies reported that FS nonpyramidal cells in neocortical areas are unresponsive to cholinergic modulation. Dentate gyrus (DG) is an independent gamma oscillator in the hippocampal formation. However, in contrast to other cortical regions, the direct impact of mAChR activation on FS BC excitability in this area has not been investigated. Here, we show that bath-applied muscarine or carbachol, two mAChR agonists, depolarize DG BCs in the acute brain slices, leading to action potential firing in the theta-gamma bands in the presence of blockers of ionotropic glutamate and γ-aminobutyric acid type A receptors at physiological temperatures. The depolarizing action persists in the presence of tetrodotoxin, a voltage-gated Na^+ channel blocker. In voltage-clamp recordings, muscarine markedly reduces background K^+ currents. These effects are mimicked by oxotremorine methiodide, an mAChR-specific agonist, and largely reversed by atropine, a non-selective mAChR antagonist, or pirenzepine, an M_1 receptor antagonist, but not by gallamine, an $M_{2/4}$ receptor antagonist. Interestingly, in contrast to M_1-receptor-mediated depolarization, M_2 receptor activation by the specific agonist arecaidine but-2-ynyl ester tosylate down-regulates GABA release at BC axons—the effect is occluded by gallamine, an M_2 receptor antagonist. Overall, muscarinic activation results in a net increase in phasic inhibitory output to the target cells. Thus, cholinergic activation through M_1-like receptor enhances BC activity and promotes the generation of nested theta and gamma rhythms, thereby enhancing hippocampal function and associated performance. © 2010 IBRO. Published by Elsevier Ltd. All rights reserved.

Key words: acetylcholine, dentate gyrus, GABAergic interneuron, basket cell, mAChR, potassium channel.

Fast rhythmic network activities in the gamma frequency band (30–80 Hz) are associated with various cognitive processes including sensory binding, selective attention and consciousness (Gray and Singer, 1989; Fries et al., 2001; Lisman and Buzsáki, 2008). In the hippocampus, gamma oscillations are commonly nested within theta (4–10 Hz) oscillations and have been implicated in learning and memory (Buzsáki, 2002; Klausberger and Somogyi, 2008; Lisman and Buzsáki, 2008). Two gamma oscillators are identified in the hippocampal formation *in vivo*: One is the dentate gyrus (DG)–hilar region and the other is the CA3–CA1 region (Csicsvari et al., 2003). Multiple lines of evidence implicate that cholinergic signaling plays an important role in nested theta-gamma rhythms. First, both principal neurons and interneurons in the hippocampus are innervated by cholinergic inputs from the medial septum/diagonal band of Broca (Frotscher and Léránth, 1985; Léránth and Frotscher, 1987; Buzsáki, 2002; Lucas-Meunier et al., 2003). Second, cholinergic agonists excite pyramidal cells as well as several specific subtypes of GABAergic cells (Lamour et al., 1982; Kawaguchi, 1997; Chapman and Lacaille, 1999; McQuiston and Madison, 1999; Fisahn et al., 2002; Lawrence et al., 2006a,b). Third, activation of muscarinic acetylcholine receptors (mAChRs) induces network gamma oscillations in the hippocampus *in vitro* (Fisahn et al., 1998; Hájos et al., 2004; Mann et al., 2005). Finally, the power of theta oscillations is reduced after ablation of cholinergic neurons of the medial septum (Lee et al., 1994) and *in vitro* gamma oscillations are absent in muscarinic M_1-receptor-deficient mice (Fisahn et al., 2002).

On the other hand, emerging evidence indicates that fast-spiking (FS), parvalbumin (PV)-expressing basket cells (BCs), are of critical importance for the generation of network oscillations (Cobb et al., 1995; Wang and Buzsáki, 1996; Bartos et al., 2001, 2002; Hájos et al., 2004; Mann et al., 2005; for review, see Bartos et al., 2007; Sohal et al., 2009). An interesting study by Monyer and her colleagues (Fuchs et al., 2007) demonstrated that reduced excitation of PV(+) BCs disrupts hippocampal gamma rhythms and hippocampal function. More recently, Sohal et al. (2009) used optogenetic technologies to further show that inhibiting PV(+) interneurons suppresses gamma oscillations *in vivo*, whereas driving these interneurons is sufficient to generate emergent gamma-frequency rhythmicity. There-

[1] These authors contributed equally to this work.

*Corresponding author. Tel: +886-2-2826-7325; fax: +886-2-2821-5307.
E-mail address: cclien@ym.edu.tw (C. C. Lien).

Abbreviations: ABET, arecaidine but-2-ynyl ester tosylate; ACh, acetylcholine; AP, action potential; BC, basket cell; CCK, cholecystokinin; DG, dentate gyrus; eIPSCs, evoked inhibitory postsynaptic currents; FS, fast-spiking; $GABA_AR$, GABA, type A receptor; GAD65, glutamate decarboxylase 65; GC, granule cell; GIRK, G-protein-coupled inwardly rectifying K^+; IC_{50}, half-maximal inhibitory concentration; IR-DIC, infrared differential interference contrast; KA, kynurenic acid; mAChR, muscarinic acetylcholine receptor; Oxo-M, oxotremorine methiodide; PV, parvalbumin; sIPSC, spontaneous inhibitory postsynaptic current; TTX, tetrodotoxin; TWIK, tandem of P domains in a weak inwardly rectifying K^+ channel.

0306-4522/10 $ - see front matter
doi:10.1016/j.neuroscience.2010.04.051

fore, cholinergic induction of gamma oscillations might be in part through direct excitation of FS BCs. However, existing evidence is at variance with this notion (for review, see Lawrence, 2008). In neocortical areas of rats, FS nonpyramidal cells are unresponsive to cholinergic neuromodulation (Kawaguchi, 1997; Porter et al., 1999; Gulledge et al., 2007; Kruglikov and Rudy, 2008), although only one study has described mAChR-mediated hyperpolarization in FS neurons (Xiang et al., 1998). Intriguingly, muscarinic responsiveness of perisomatic inhibitory interneurons (including BCs) in the CA1 region seems quite heterogeneous (McQuiston and Madison, 1999). Roughly half the interneurons whose axons they classified as perisomatic are depolarized or oscillated in response to muscarine, whereas the remainder shows no response (McQuiston and Madison, 1999).

Despite the essential role of PV(+) FS BCs in the gamma oscillations, no attempts have been made so far to examine the functional impact of mAChR activation on PV(+) FS BC excitability in the DG. Therefore, a major goal of this study is to investigate the impact of postsynaptic mAChR activation on rigorously identified FS BCs in the DG of rat brain slices. In sharp contrast to FS BCs in other cortical regions, our work reveals a robust relationship between mAChR activation and FS cell excitation. Activation of M_1 receptors results in somatic membrane depolarization, an increase in input resistance, and enhancement of spike outputs. Functionally, M_1 receptor activation in BCs not only leads to a net increase in GABAergic inhibitory tones in targeted granule cells (GCs) but likely also provides a tonic driving force required for interneuron network synchronization.

EXPERIMENTAL PROCEDURES

Preparation of hippocampal slices

Transverse hippocampal slices (300 μm thick) were prepared from male Sprague–Dawley rats [postnatal day 16 (P16)–P21] using a vibrating tissue slicer (DSK-1000, Dosaka, Kyoto, Japan) as described previously (Lien et al., 2002; Lien and Jonas, 2003). Animals were sacrificed by decapitation in agreement with national and institutional guidelines and all procedures were approved by the Animal Care and Use Committee of the National Yang-Ming University. Slices were sectioned in the ice-cold cutting saline containing (in mM): 87 NaCl, 25 $NaHCO_3$, 1.25 NaH_2PO_4, 2.5 KCl, 10 glucose, 75 sucrose, 0.5 $CaCl_2$ and 7 $MgCl_2$. Following sectioning, slices were incubated in the cutting saline (oxygenated with 95% O_2/5% CO_2) in a holding chamber at 34 °C for 25 min, and then at room temperature until used. During experiments, an individual slice was transferred to a submersion recording chamber and was continuously superfused with oxygenated artificial cerebrospinal fluid containing (in mM): 125 NaCl, 25 $NaHCO_3$, 1.25 NaH_2PO_4, 2.5 KCl, 25 glucose, 2 $CaCl_2$ and 1 $MgCl_2$.

Electrophysiology

Patch pipettes for recordings were pulled from borosilicate glass tubing (outer diameter 1.5 mm, inner diameter 0.86 mm; Harvard apparatus, Holliston, MA, USA) and heat-polished before used. The pipette resistance ranged from 3 to 7 MΩ. Experiments were performed under visual control using an infrared differential interference contrast (IR-DIC) microscope (BX51WI, Olympus, Tokyo, Japan). DG BCs were visually identified by the size and the location of cell body at the GC layer–hilus border under IR-DIC optics (Hefft et al., 2002; Aponte et al., 2008). Only neurons that generated ≥70 action potentials (APs) per second and had input resistance <150 MΩ during 1-s current injections at 24 °C were selected for experiments. For experiments at 36 °C, neurons that fired ≥100 Hz and exhibited low input resistance (<100 MΩ) were chosen. Young and mature granule cells were arbitrarily defined according to their input resistance. Young granule cells having higher input resistance (R_{in}>1 GΩ) than mature granule cells (R_{in}<1 GΩ) (Stocca et al., 2008). Whole-cell patch recordings were made as described previously (Lien et al., 2002; Lien and Jonas, 2003), using Multiclamp 700B or Axopatch 200B amplifiers (Molecular Devices, Union City, CA, USA). Pipette capacitance was compensated. Series resistance (12–38 MΩ) was compensated to 100% in current-clamp configuration and to 80% in voltage-clamp configuration during measurements of reversal potentials. For synaptic responses, evoked inhibitory postsynaptic currents (eIPSCs) were induced by a glass stimulation pipette (~20 μm tip diameter) placed in the GC layer. Pulses were delivered by using a stimulus isolator and had an amplitude of 2–7 V and a duration of 100 μs. The stimulation frequency was 0.2 Hz. Experiments in which the series resistance changed by >15% were discarded. Signals were low-pass filtered at 4 kHz (four-pole Bessel), and sampled at 10 kHz using the Digidata 1440 (Molecular Devices); data acquisition and pulse generation were performed using pClamp 10.2 (Molecular Devices). Recordings were made at 22–24 °C, unless otherwise specified.

Single-cell RT-PCR

Expression of PV was analyzed using single-cell RT-PCR approach as previously described (Lien et al., 2002). RNase-free patch-clamp buffer containing (mM): 140 KCl, 3 $MgCl_2$, 5 Hepes, 5 EGTA (pH=7.3) was autoclaved before used. Patch-clamp capillaries were baked overnight at 220 °C prior to use. The cytoplasm of a recorded neuron was harvested into the recording pipette under visual control without losing the gigaseal immediately after electrophysiological characterization. The contents of the patch pipette (~3 μl) were expelled into a 0.2-ml PCR tube (Axygen Scientific, Union city, CA, USA) containing 7 μl reverse transcription (RT) mix (SuperScript III, Invitrogen). The mix contained 1 μl diethylpyrocarbonate (DEPC)-treated water, 5 μl 2× RT reaction mix (oligo$(dT)_{20}$, random hexamers, $MgCl_2$ and dNTPs) and 1 μl RT enzyme mix (SuperScript III RT and recombinant ribonuclease inhibitor). Total volume was about 10 μl. After a series of incubation at recommended temperatures according to Invitrogen's optimized protocol for RT, the cDNA-containing tube was stored at −70 °C until used.

Following cDNA synthesis, the cDNA solution of a single cell was split into three aliquots (5 μl). Each was used for the amplification of a single gene. A PCR approach with MyCycler (Bio-Rad, Hercules, CA, USA) was performed in a total volume of 20 μl with 1 μl of 10 μM primers (each), 5 μl DEPC-treated water and the PCR mix (TakaRa, Shiga, Japan) containing (μL): 0.2 *Taq* DNA polymerase, 1.6 dNTP, 2 10× buffer, 9.2 water. Primers were designed with Perlprimer v1.1.14 and selected for maximal specificity and intron-overspanning amplicons. PV (GenBank accession NM_022499.2) was detected with a pair of primers GGCGATAGGAGCCTTTACTGCTGC (forward) and GAAACCCAGGAGGGCCGCGA (reverse), which gave a PCR product of 372 bp. Cholecystokinin (CCK) (GenBank accession NM_012829.1) was detected with a pair of primers GCTGGACAGCAGCCGTTGGA (forward) and GGCCAGAGGGAGCTTTGCGG (reverse), which gave a PCR product of 280 bp. Glutamate decarboxylase 65 (GAD65) (GenBank accession NM_012563.1) was detected with a pair of primers TGGCATCTCCGGGCTCTGGCT (forward) and TGGCAGCAGGTCTGTTGCGTGG (reverse), which gave a PCR product of 296 bp. The molecular weights of all amplicons

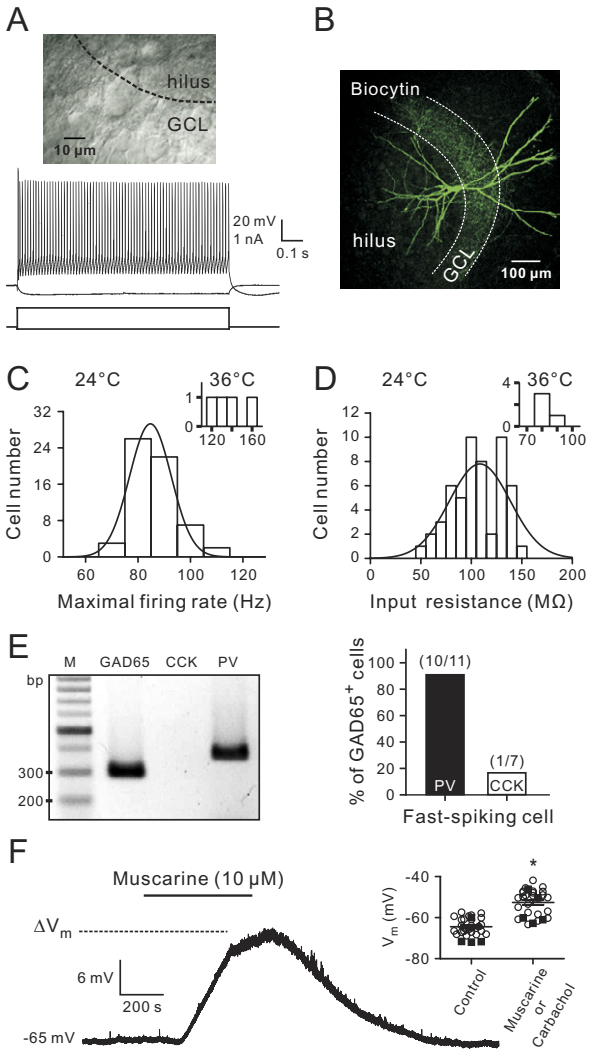

Fig. 1. Muscarine excited fast-spiking cells in the DG. (A) Top, IR-DIC image of a BC near the border (dashed line) between the GC layer (GCL) and the hilus in the DG. Middle, voltage responses of the same BC to 1 s de- or hyperpolarizing current pulses in the whole-cell current-clamp configuration at 24 °C. Membrane potential before the pulse was held at −70 mV. Currents during the pulse were +0.9 and −0.1 nA. Bottom, protocol for current pulses. (B) Two-photon *z*-stack (maximal intensity) projection of the same BC in (A) filled with biocytin during whole-cell recording and stained with FITC-conjugated avidin. The axonal ramification is almost exclusively within the GCL. Dashed lines demarcate the borders of GCL. (C) Maximal firing rates obtained from 60 rigorously identified BCs at 24 °C in response to 1-s depolarizing pulse (600–900 pA). Inset, data obtained at 36 °C. Distribution of maximal firing rates was fitted with a Gaussian function, yielding the mean of 84.7 and the standard deviation of 7.9. (D) Input resistance obtained from the same population of BCs shown in (C) at 24 °C. Distribution of data was fitted with a Gaussian function, yielding the mean of 108.5 and the standard deviation of 30.3. Inset, data obtained at 36 °C. (E) Left, Ethidium Bromide-stained gels of the PCR products amplified with primers specific for PV, CCK and GAD65 transcripts. Molecular weight marker (M) was shown in the left lane, together with the corresponding number of base pairs. All neurons (n=11) analyzed were positive for GAD65, indicating selective harvesting from GABAergic interneurons. Right, bar plot showing the percentage of PV- and CCK-expressing cells from all GAD65$^+$ cells. (F) Bath-applied muscarine (10 μM) at 24 °C induced marked membrane depolarization of a fast-spiking BC in the presence of KA (2 mM), gabazine (1 μM) and TTX (0.5 μM). Inset, summary plot of the membrane potential before and after addition of muscarine (open circles) or carbachol (filled boxes). * $P<0.05$. For interpretation of the references to color in this figure legend, the reader is referred to the Web version of this article.

were subsequently examined on Ethidium Bromide-stained agarose gels; sizes were in close agreement with the expected length (Fig. 1E). To exclude the possibility of contaminations, no template control was performed in parallel to every PCR, and the reverse transcriptase was omitted in a subset of cells. Additional controls to exclude non-specific harvesting were performed by advancing pipettes into the slice and taking them out without seal formation and suction.

Solutions and drugs

The intracellular solution for BC recording consisted of (in mM): 135 Kgluconate, 20 KCl, 0.1 EGTA, 2 $MgCl_2$, 4 Na_2ATP, 10 Hepes and 0.3 Na_3GTP; For GC recording, it consisted of (in mM): 35 Kgluconate, 100 KCl, 10 EGTA, 2 $MgCl_2$, 2 Na_2ATP, 10 Hepes and 0.3 Na_3GTP; pH adjusted to 7.3 with HCl or KOH. Kynurenic acid was from Sigma (St. Louis, MO, USA) and Ascent Scientific (Weston super Mare, UK); gabazine was from Tocris Bioscience (Park Ellisville, MO, USA) and Ascent Scientific; tetrodotoxin (TTX) was from Tocris Bioscience. All other chemicals were from Sigma except where noted.

Post hoc identification of BC morphology

Neurons were filled with biocytin (1–2 mg/mL) during whole-cell recordings and subsequently fixed overnight with 4% paraformaldehyde in phosphate-buffered solution (PB; 0.1 M, pH 7.3). After washing with PB, slices were incubated with fluorescein isothiocyanate (FITC)-conjugated avidin-D (2 μl/mL; Invitrogen, Eugene, OR, USA) in PB and 0.3% Triton X-100 overnight at 4 °C. After wash, slices were embedded in mounting medium Vectashield® (Vector Laboratories, Burlingame, CA, USA). Labeled BCs were examined by a two-photon microscope using a pulsed titanium: sapphire laser (Chameleon-Ultra II tuned to 800 nm; Coherent, Portland, OR, USA) attached to a Leica DM6000 CFS microscope (Leica, Wetzlar, Germany) that was equipped with a 20×/0.5 numerical aperture (NA) water immersion objective (HCX APO L; Leica, Wetzlar, Germany). The morphologies of the cells were reconstructed from a stack of 350–600 images (voxel size, 1.4–1.6 μm in the *x*-*y* plane; 0.24–0.5 μm along the *z*-axis) and an example of a reconstructed BC was shown in Fig. 1B.

Data analysis and statistics

Data were analyzed using Clampfit 10.2 (Molecular Devices) and Sigma plot 10.0 (Systat Software, Point Richmond, CA, USA). MiniAnalysis (6.0.3 Synaptosoft, Fort Lee, NJ, USA) was used to detect and analyze spontaneous IPSCs (sIPSCs). The concentration-response curve was fitted with the function:

$$f(c) = \frac{1}{\left[1+\left(\frac{IC_{50}}{c}\right)^{n}\right]} \quad (1)$$

where c denotes the concentration, IC_{50} represents the half-maximal inhibitory concentration, and n denotes the Hill coefficient. For the measured reversal potentials, data points of *I*–*V* relations were fitted by 2nd order polynomials, from which the interpolated potentials were calculated. The equilibrium potential of K^+ channels (E_k) was predicted by the Nernst equation (Hille, 2001):

$$E_k = \frac{RT}{F} \ln \left(\frac{[K^+]_o}{[K^+]_i}\right) \quad (2)$$

where $[K^+]_o$, $[K^+]_i$ are outer and inner K^+ concentrations and F, R, T have standard thermodynamic meanings (Hille, 2001).

AP voltage threshold was determined from the first sampling point when AP trajectory exceeds 50 V/s as described previously (Kole and Stuart, 2008). Values indicate mean±standard error of the mean (SEM) unless otherwise stated. Error bars in figures also represent SEM. Statistical significance was tested by the non-parametric Wilcoxon signed-rank test, Wilcoxon rank-sum test or Kolmogorov–Smirnov test (for cumulative probability plots in Fig. 7) at the significance level (P) indicated, using GraphPad Prism 5.0 (La Jolla, CA, USA) or MiniAnalysis.

RESULTS

Muscarinic agonists induce *in vitro* gamma oscillations in the hippocampus (Fisahn et al., 1998; Hájos et al., 2004; Mann et al., 2005). Given the important role of BCs in gamma oscillations, we tested the direct muscarinic action on FS BC excitability in the DG of the rat hippocampus.

Muscarinic depolarization of fast-spiking basket cells

FS BCs in the DG of acute brain slices were identified based on the location of their cell bodies near the border between GC layer and hilus (Aponte et al., 2006, 2008; Doischer et al., 2008) (Fig. 1A, top), high-frequency AP phenotypes, relatively low input resistance and the absence of sag response upon hyperpolarizing current pulses at 24 °C (Fig. 1A, bottom). Only neurons that generated ≥70 APs per second and had input resistance <150 MΩ were selected for experiments. As shown in Fig. 1B, we chose cells with axonal arbors largely restricted to the GC layer for subsequent analysis. The maximal firing rates and input resistance from 60 morphologically confirmed BCs were 82±1 Hz (Fig. 1C) and 107±4 MΩ (Fig. 1D), respectively. Results obtained at 36 °C from four morphologically confirmed BCs were also shown for comparison (Fig. 1C, D insets). In a subset of recorded neurons, the expression of the GAD65, PV, CCK was detected using single-cell RT-PCR (Fig. 1E left). The majority (10 out 11 cells) of GAD65-expressing FS cells was immunoreactive for PV, whereas only one out of seven GAD65-expressing FS cells was CCK-positive (Fig. 1E right).

To determine the postsynaptic cholinergic action on BCs, we investigated the effect of bath-applied mAChR agonist muscarine on BC excitability (Fig. 1F). We recorded BCs in the whole-cell current-clamp recording in the presence of kynurenic acid (KA, 2 mM), a broad-spectrum blocker of ionotropic glutamate receptors, gabazine (1 μM), a GABA receptor type A ($GABA_AR$) antagonist, and TTX (0.5 μM), a voltage-gated Na^+ channel blocker. TTX was used to block the discharge of the recorded neuron as well as the network activity. A representative experiment showed that muscarine (10 μM) reversibly induced slow membrane depolarization of a FS BC by 13.5 mV at 24 °C (Fig. 1F). The effect of muscarine on BC membrane potential was similar to that of another cholinergic agonist carbachol (25 μM) (muscarine, 12.1±0.8 mV, n=24; carbachol 10.8±1.4 mV, n=5; P=0.69, Wilcoxon rank-sum test; Fig. 1F inset) and thus they were pooled together for analysis. Taken together, both muscarine and carbachol produced significant depolarization (ΔV_m=11.9±0.7 mV, n=24 for muscarine and 5 for carbachol; P<0.05) of all recorded FS interneurons.

Muscarinic effect on BC firing patterns

To determine whether muscarine-mediated depolarization was sufficient to induce BC firing, we performed similar experiments in the absence of TTX. In the presence of KA and gabazine, FS BCs exhibited slow depolarization (ΔV_m=11±1 mV, n=17; P<0.05) followed by repetitive firing in response to muscarine at 24 °C (Fig. 2A). A part of spike train in Fig. 2A was expanded and shown in Fig. 2B. Analysis of the spike train revealed a rhythmic bimodal firing pattern, which consists of beta (10–25 Hz) frequency spike bursts with inter-burst frequency in the theta (1–5 Hz) range (Fig. 2B). The bimodal firing patterns at 24 °C were shifted to multimodal firing patterns at 36 °C (ΔV_m=16±2 mV, n=10; P<0.05) (Fig. 2C), which covered a wide range of frequencies, from slow theta (3–8 Hz) and beta (10–30 Hz) ranges to the fast gamma (30–80 Hz) frequency band (Fig. 2D).

Muscarinic excitation was associated with a reduced rheobase

We next determined if the muscarinic effect on BC excitability persisted when the cell was maintained at a similar voltage (−72 mV) as in the control by adjusting the holding current throughout the experiment. Under control conditions and in the presence of muscarine, BCs were depolarized by a series of incremental current steps (1 s duration, 2 pA step) (Fig. 3A). As shown in Fig. 3A–C, BCs did not generate spikes in response to a 1-s current pulse (300 pA) injection in the control (Fig. 3A top), but displayed a single spike in response to a relatively smaller current pulse (266 pA) in the presence of muscarine (Fig. 3A bottom, black). The overlay of both voltage trajectories revealed that muscarine moderately increased the input resistance as measured during small depolarizing current steps. The plot of spike number against current pulse showed that muscarine significantly lowered the current threshold (rheobase) for spike generation (Fig. 3B, arrows indicate the rheobase values), but had no effect on the mean AP frequency in response to the large current pulse (500 pA) injection (control, 52.8±5.5 Hz, n=5 and muscarine, 46.4±6.5 Hz; n=5, P=0.14; Fig. 3C). Interestingly, in contrast with the current threshold, the AP voltage threshold (control, −36.8±0.8 mV and muscarine, −34.2±0.8 mV; n=7, P<0.05; see experimental procedures) was slightly higher in the presence of muscarine than the control. Overall, the AP frequency evoked by the 1-s long pulse (500 pA) was not changed by muscarine while the rheobase (280±41 pA) was significantly reduced by muscarine to 84% (234±45 pA; n=6; P<0.05) of the control (Fig. 3D).

Inhibition of resting K^+ conductance by muscarine

Muscarine may depolarize neurons *via* inhibition of resting K^+ conductance (Nicoll, 1988). We tested this possibility by recording the resting current change after bath addition

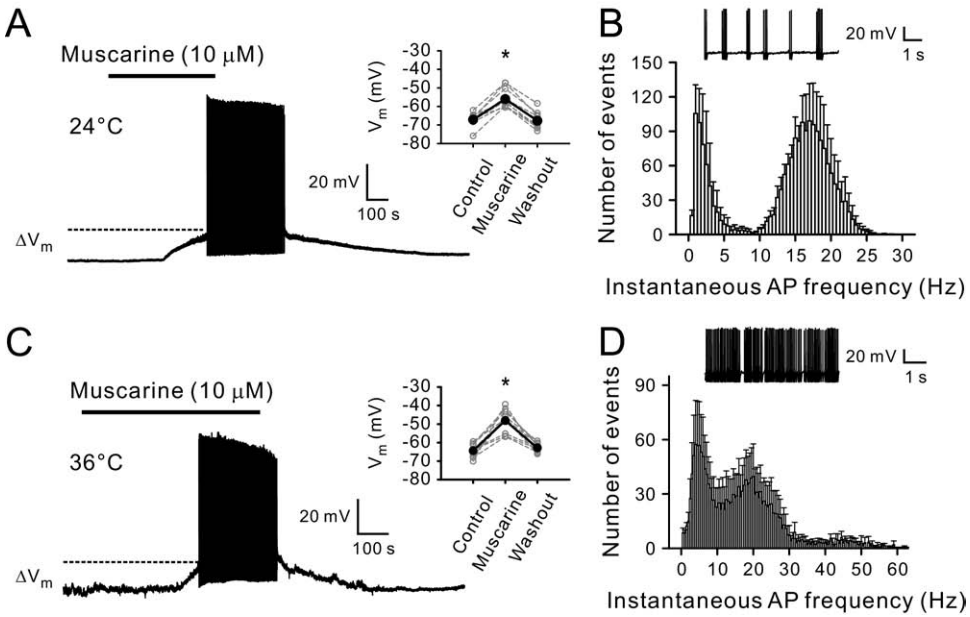

Fig. 2. Muscarine induced firing of BCs. (A) Bath-applied muscarine (10 μM) induced membrane depolarization (ΔV_m) followed by repetitive firing in the presence of KA (2 mM) and gabazine (1 μM) at 24 °C. Inset is the summary of muscarinic effect on V_m from 17 BCs. Black circles indicate mean; gray circles indicate data from individual experiments. Measurements from the same cell are shown connected by lines. * $P<0.05$. (B) Representative trace of expanded spike train in the presence of muscarine at 24 °C. Histogram of instantaneous AP frequency in the presence of muscarine from four BCs. (C) Muscarine (10 μM) induced membrane depolarization followed by firing at 36 °C under the same condition as in (A). Inset is the summary of muscarinic effect on V_m from 10 BCs. * $P<0.05$. (D) Representative trace of expanded spike train in the presence of muscarine at 36 °C. Histogram of instantaneous AP frequency in the presence of muscarine from eight BCs.

of muscarine. A representative experiment showed that muscarine at a concentration of 1–100 μM changed the holding current in a concentration-dependent manner when a BC was voltage clamped at −65 mV (Fig. 4A top). The holding current gradually decreased from +40 pA (outward) to −40 pA (inward) upon increasing concentrations of muscarine, reflecting either the induction of an inward current or the blockade of an outward current by muscarine. The change of holding current was concomitant with an increase of input resistance (Fig. 4A bottom), suggesting the blockade of an outward current. The plot of muscarine concentration against the relative decrease of holding current (normalized by the effect of 100 μM muscarine) was fitted with a single Hill equation, yielding a half-maximal inhibitory concentration (IC_{50}) of 5.1 μM and a Hill coefficient of 1.1 ($n=3$ for each symbol, Fig. 4B).

Activation of mAChRs may result in inhibition of diverse populations of K^+ channels including inward rectifier K^+ channels, KCNQ/M/Kv7 channels, calcium-activated K^+ channels, and leakage K^+ channels (McQuiston and Madison, 1999; Watkins and Mathie, 1996; Lawrence et al., 2006b,c; Mathie, 2007). To investigate the functional properties of mAChR-mediated currents, we applied a voltage ramp protocol (from −40 to −120 mV, 0.8 V/s) to BCs before and after bath addition of muscarine in the voltage-clamp configuration (Fig. 4C). Consistent with previous reports (McQuiston and Madison, 1999; Lawrence et al., 2006b), a representative data showed that muscarine-sensitive current obtained by subtracting the current in the presence of muscarine from the control had a reversal potential of −103 mV, close to the K^+ equilibrium potential −106 mV (Fig. 4D). Overall, the current (I)–voltage (V) relationship of muscarine-sensitive currents appeared quasi-linear (ohmic) with a reversal potential of −109±3 mV (Fig. 4E, $n=3$). Finally, we examined the possible occlusion between the effect of muscarine and the effect of barium, a broad-spectrum resting K^+ channel blocker. Muscarine (10 μM) and barium (1 mM), known to block 2P domain K^+ and inward rectifying K^+ channels, induced −60.0±6.9 pA ($n=29$) and −64.6±27.1 pA ($n=4$) changes of holding current, respectively (Fig. 4F). Coapplication of muscarine (10 μM) and barium (1 mM) induced −97.0±31.6 pA ($n=5$) change of the holding current, not only markedly less than the arithmetic sum of individual effects, but also not significantly different from the effect of each of the blockers ($P>0.05$; Wilcoxon rank-sum test). Thus the results showed a large degree of occlusion between the effects of muscarine and barium.

M_1 receptors mediated BC depolarization

There are five subtypes of mAChR receptors (M_1 to M_5), with M_1, M_2 and M_4 being the predominant receptors in the hippocampus (Volpicelli and Levey, 2004). GABAergic inhibitory interneurons of the hippocampus are major targets of septal cholinergic fibers (Frotscher and Léránth, 1985; Léránth and Frotscher, 1987; Parra et al., 1998; Lawrence et al., 2006a,b). We next examined the subtypes of mAChRs that mediated the depolarizing effect on BCs using the pharmacological approach. First, we found that bath-applied atropine (1 μM), a broad-spectrum mAChR receptor antagonist, largely reversed the muscarine-medi-

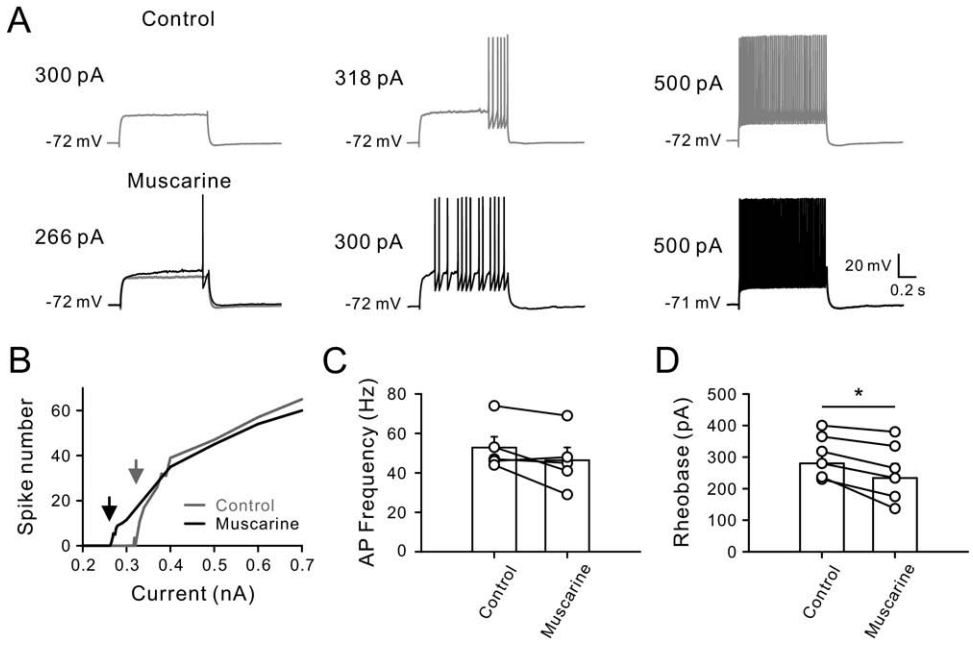

Fig. 3. Muscarinic excitation was associated with a reduced rheobase. (A) A series of incrementing current pulses depolarized a BC in the control (top) and in the presence of 10 μM muscarine (bottom). For the comparison, the voltage response (gray) to the 300 pA current pulse in the control was overlaid with that (black) to the 266 pA current pulse in the presence of muscarine. (B) Relationship of spike number against injected current from the same BC in (A). Arrows indicate the rheobase required for spike generation during a 1-s current pulse in the control and in the presence of muscarine, respectively. (C) The number of APs during a 1-s depolarizing (500 pA) was not significantly changed ($P>0.1$) after addition of muscarine. (D) Rheobase was significantly reduced after bath application of muscarine (10 μM). * $P<0.05$.

ated effect (Fig. 5A). In accordance with this notion, bath application of Oxo-M (10 μM), an mAChR-selective agonist, led to a decrease of the holding current of the BCs (Fig. 5B). Furthermore, the muscarine-mediated response was largely reversed by the bath addition of pirenzepine, an M_1 receptor antagonist, at a low concentration (1 μM), indicating that the muscarinic effect was mainly mediated by M_1-like mAChRs (Fig. 5C). Finally, the bath-applied $M_{2/4}$ receptor antagonist gallamine (2 μM) did not significantly attenuate the effect of muscarine (Fig. 5D). The graphs (Fig. 5E–H) summarized the results of pharmacological characterization of the muscarine-induced holding current changes in FS interneurons.

Presynaptic M_2 receptor activation down-regulated GABA release

Activation of mAChRs down-regulates GABA release of FS BCs (Hefft et al., 2002; Kruglikov and Rudy, 2008) likely through presynaptic M_2 receptors (Hájos et al., 1998). We thus explored whether M_1- and M_2-like receptors were differentially expressed in FS BCs. To investigate presynaptic M_2 receptor-mediated effects, we recorded pharmacologically isolated monosynaptic IPSCs in GCs by extracellularly stimulating BC axons in the GC layer (Fig. 6A). Arecaidine but-2-ynyl ester tosylate (ABET, 30 μM), a preferential muscarinic M_2 receptor agonist, significantly inhibited eIPSCs (Fig. 6B–D). Furthermore, pretreatment with gallamine (10 μM), a muscarinic M_2 receptor antagonist, prevented ABET-mediated inhibition of GABA release (Fig. 6E, F). Most notably, gallamine significantly increased eIPSCs, suggesting tonic inhibition of GABA release in BCs by endogenous ACh (Fig. 6E, F). Taken together, these results are consistent with the previous studies that mAChRs play an auto-regulatory role at axon terminals of BCs and further provide direct evidence supporting the hypothesis that expression of M_2-type receptors at BC axons.

Muscarinic facilitation on GABAergic transmission

Our results showed that M_1 receptor activation robustly enhanced FS BC excitability, whereas M_2 receptor activation down-regulated GABA release of the same cell. How the dichotomous effects mediated by M_1- and M_2-like receptors in BCs affected the net inhibitory outputs? To address this question, we recorded sIPSCs from GCs in the presence of KA (2 mM) (Fig. 7A, inset). The input resistance and intrinsic membrane properties of young GCs were shown to correlate well with the dendritic development (Stocca et al., 2008). In this study, we first recorded sIPSCs from young GCs (defined by input resistance >1 GΩ) (Stocca et al., 2008), because young GCs at this stage exclusively receive inputs from somatic GABAergic synapses (Ming and Song, 2005; Stocca et al., 2008). A representative experiment (Fig. 7A) showed that bath-applied muscarine (10 μM) profoundly increased sIPSCs in a young GC (1.2 GΩ) at holding potential of -65 mV. The increased IPSCs were sensitive to 1 μM gabazine, suggesting that the increased synaptic events were $GABA_A$R-mediated IPSCs (Fig. 7A). The plots of cumulative distribution showed that muscarine alone greatly en-

Fig. 4. Muscarine resulted in inhibition of K^+ currents of BCs. (A) Top, bath-applied muscarine (1–100 μM) markedly decreased the resting current of a BC at the holding voltage of −65 mV in the presence KA (1–2 mM) and gabazine (1 μM). Bottom, the input resistance was concomitantly increased during muscarine application. (B) Dose-response curve of muscarinic effect on the holding currents from three BCs. Open symbols were fitted with a single Hill equation, yielding an IC_{50} of 5.1 μM and a Hill coefficient of 1.1. (C) Top, representative currents of a BC evoked by a voltage ramp in the control (black) and in the presence of muscarine (grey), respectively. The dashed line indicates zero current. Bottom, a voltage ramp protocol from −40 to −120 mV with the rate of 0.8 V/s. (D) *I–V* relationship of the muscarine-sensitive current obtained by subtracting the current in the presence of muscarine from that in the control in a single BC revealed a reversal potential of −103 mV. (E) Averaged *I–V* relationship of the muscarine-sensitive current obtained from three BCs. (F) Bar graph showing changes of holding current by 10 μM muscarine (n=29), 1 mM barium (n=4) and a combination of 10 μM muscarine and 1 mM barium (n=5). Note marked occlusion of the effects.

hanced the frequencies of sIPSCs by ~23 fold (control, 0.13 Hz; muscarine, 3.09 Hz; $P<0.001$; Kolmogorov–Smirnov test; Fig. 7B) without altering sIPSC amplitudes (control, 21.9±2.0 pA; muscarine 27.3±1.0 pA; $P=0.28$; Kolmogorov–Smirnov test; Fig. 7C). On the contrary, further addition of gabazine (1 μM) markedly decreased the frequencies (muscarine, 3.09 Hz; muscarine+gabazine, 0.02 Hz; $P<0.001$; Kolmogorov–Smirnov test; Fig. 7B) as well as amplitudes of sIPSCs (muscarine, 27.3±1.0 pA; muscarine+gabazine, 13.8±1.4 pA; $P<0.05$; Kolmogorov–Smirnov test; Fig. 7C).

Notably, a similar scenario was also found in mature GCs (defined by input resistance <1 GΩ), although the effect on sIPSC frequency was substantially less than that in young GCs. Overall, muscarine markedly enhanced the frequency (young GCs: control, 0.30±0.05 Hz; muscarine, 1.90±0.43 Hz; $n=10$, $P<0.0005$; Fig. 7D; mature GCs: control, 1.95±0.34 Hz; muscarine, 4.00±0.80 Hz; $n=12$, $P<0.05$; Wilcoxon signed-rank test; Fig. 7F) but did not alter the mean amplitude (young GCs: control, −20.1±1.4 pA; muscarine, −26.8±7.4 pA; $n=10$, $P=0.91$; Fig. 7E; mature GCs: control, −20.6±1.7 pA; muscarine, −21.4±

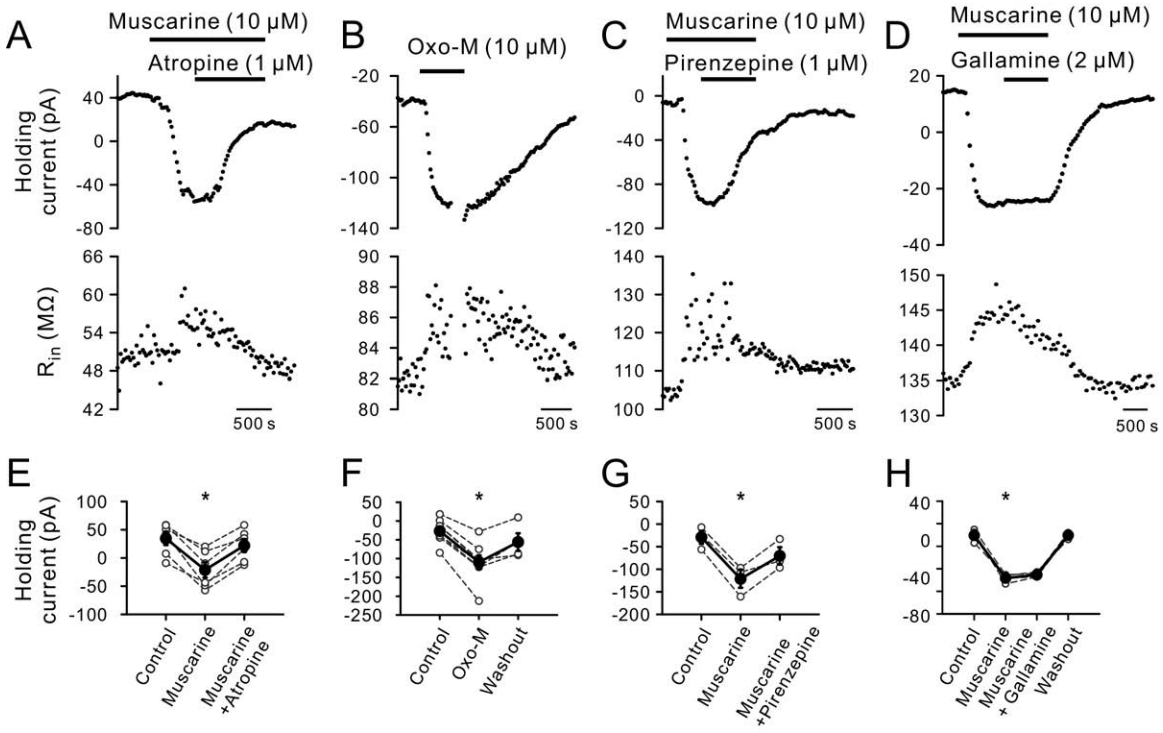

Fig. 5. M_1 receptor stimulation reduced background K^+ conductance. (A) Top, the muscarine-mediated effect on the holding current of a BC was largely reversed by atropine (1 μM), an mAChR receptor antagonist (top). Bottom, the input resistance (R_{in}) was concomitantly changed with the holding current. (B) Top, Oxo-M (10 μM), an mAChR receptor agonist, had a similar effect on the holding current of a BC. Bottom, the R_{in} was concomitantly changed with the holding current. (C) Pirenzepine (1 μM), an M_1 subtype mAChR antagonist, largely reversed the effect of muscarine (10 μM) on the holding current of a BC (top) and the R_{in} (bottom). (D) The muscarinic effect on the holding current (top) and the R_{in} (bottom) persisted in the presence of the $M_{2/4}$ antagonist gallamine (2 μM). (E–H) Summarized effect of muscarine, atropine, Oxo-M, pirenzepine and gallamine on holding currents of BCs. * $P<0.05$.

1.9 pA; $n=12$, $P=0.81$; Wilcoxon signed-rank test; Fig. 7G) of sIPSCs recorded from both young and mature GCs.

DISCUSSION

Cholinergic modulation of DG FS interneurons

Several studies reported that ACh profoundly alter excitability of pyramidal cells and GABAergic interneurons in the hippocampus and other brain regions (Lamour et al., 1982; Behrends and ten Bruggencate, 1993; Kawaguchi, 1997; Scuvée-Moreau et al., 1998; Chapman and Lacaille, 1999; McQuiston and Madison, 1999; Fisahn et al., 2002; Lawrence et al., 2006a,b). Despite its diverse cellular and synaptic targets, the muscarinic actions on cortical or hippocampal interneurons are highly specific, altering the excitability of distinct inhibitory cell types (reviewed by Lawrence, 2008). In frontal cortex, muscarinic agonists selectively modulate the activities of peptide (somatostatin or vasoactive intestinal polypeptide)-containing GABAergic cells with regular- or burst-spiking characteristics (Kawaguchi, 1997). In the hippocampus, interneurons near the border between stratum radiatum and stratum lacunosum-moleculare (LM) of CA1 area are depolarized by bath application of carbachol and the depolarization is sufficient to induce rhythmic AP generation (Chapman and Lacaille, 1999). Similarly, mAChR activation depolarizes CA1 stratum oriens interneurons and tunes them to amplify spike reliability during theta rhythmic inputs (Lawrence et al., 2006a).

However, earlier studies have shown that the excitability of FS cells in neocortex is affected little by ACh and other neuromodulators (Kawaguchi, 1997; Gulledge et al., 2007; Kruglikov and Rudy, 2008), leading to the view that these cells tend to operate as a constant “clockwork” for cortical network oscillations (reviewed in Freund and Katona, 2007; also see Discussion in Kruglikov and Rudy, 2008). Here, in contrast with previous investigations in FS cells in other cortical regions, our results demonstrate that cholinergic system has direct excitatory influence on these interneurons in the DG and thus provide a piece of evidence for region-specific cholinergic modulation of BCs.

Differential expression of M_1- and M_2-like receptors in FS BCs

M_1 receptors are known to play a prominent role in the depolarizing effect on hippocampal CA1 pyramidal cells (Nishikawa et al., 1994; Scuvée-Moreau et al., 1998). Consistent with prior reports, the IC_{50} value (5 μM) of muscarine measured in the present study is comparable to those measured in CA1 pyramidal cells (8.6 μM by Nishikawa et al., 1994; 0.7 μM by Scuvée-Moreau et al., 1998). Taken

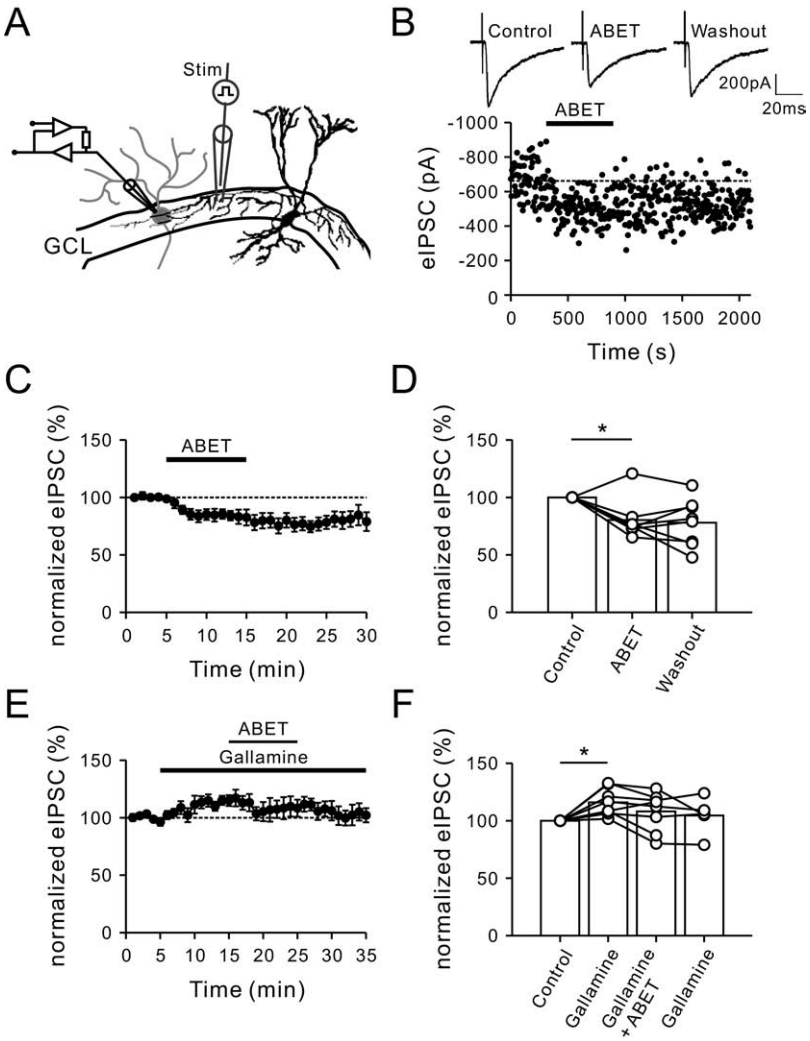

Fig. 6. Presynaptic M_2 receptor mediated inhibition of GABA release. (A) Schematic illustration of experimental configuration. (B) Example of 30 μM ABET-mediated inhibition of eIPSCs at BC-GC synapses. Traces of eIPSCs were average of 30–60 sweeps. Peak amplitudes of eIPSCs (V-clamp −70 mV) were plotted against time. Dashed line indicated the mean amplitude (baseline) before ABET application. (C) Summary of results from experiment similar to that in (B). Peak amplitudes of eIPSCs were normalized to the baseline and averaged from eight cells. (D) Bar graph showing normalized peak amplitude of eIPSCs in the control, after bath application of ABET and washout. * $P<0.05$. (E) Pretreatment of 10 μM gallamine induced an increase of eIPSCs and prevented inhibitory effect of ABET. Data were obtained from five cells. (F) Bar graph showing normalized peak amplitude of eIPSCs in the control, pretreatment of gallamine, after gallamine+ABET and after ABET washout. * $P<0.05$.

together with the high sensitivity to pirenzepine, our results point to M_1-like-receptor-mediated down-regulation of K^+ currents in BCs.

Direct activation of mAChRs in FS axon terminals is shown to down-regulate GABA release in the DG and neocortex (Hefft et al., 2002; Kruglikov and Rudy, 2008). Consistently, we found that ABET, a preferential M_2 receptor agonist, down-modulated GABA release of BCs (Fig. 6B–D). Thus, specific subcellular localization of M_1- and M_2-like receptors in BCs (Frotscher and Léránth, 1985; Hájos et al., 1998; Hefft et al., 2002; Kruglikov and Rudy, 2008) may account for the dichotomous effects of mAChR activation. By local release at specific subcellular domains, ACh might serve as a bi-functional neuromodulator in the regulation of BC excitability and GABA release.

Modulation of background K^+ conductances through mAChR activation

Hippocampal interneurons are highly sensitive to neuromodulators by expressing a rich repertoire of neurotransmitter receptors (Parra et al., 1998; Gorelova et al., 2002; Kruglikov and Rudy, 2008). As a general view, multiple metabotropic receptors can be expressed by a single interneuron (Nicoll, 1988; Parra et al., 1998; Hefft et al., 2002; Kruglikov and Rudy, 2008) and a given receptor can affect multiple molecular targets (Nicoll, 1988; Lawrence et al., 2006a). On the contrary, multiple metabotropic receptors can also affect the same molecular target (Nicoll, 1988; Talley et al., 2000). In the present study, mAChR activation reduces the holding currents of BCs in the volt-

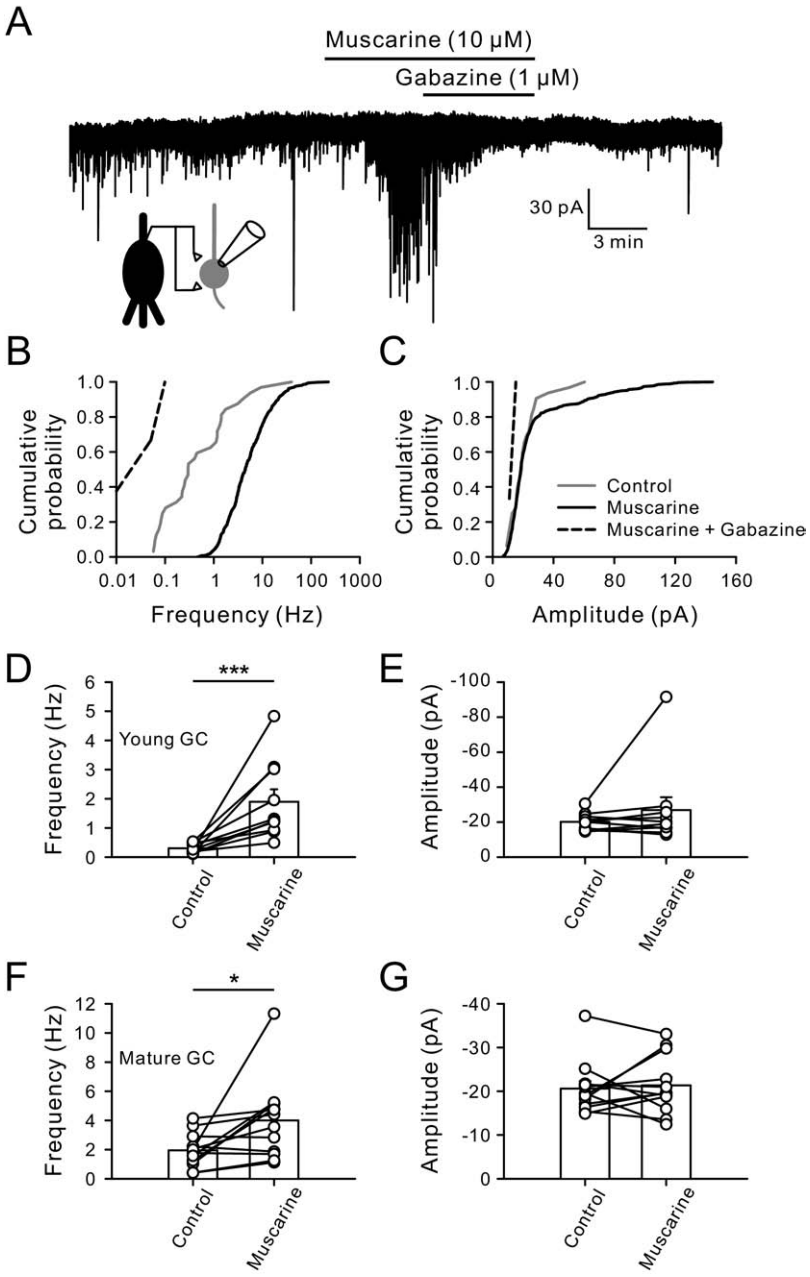

Fig. 7. Muscarine enhanced $GABA_A$R-mediated currents in GCs. (A) Inset, a schematic drawing of the experimental arrangement showing that a young GC receives major axosomatic synapses from BCs; a representative recording showing the effect of muscarine on sIPSCs recorded at holding potential of −65 mV from a young GC with input resistance of 1.2 GΩ before and after bath application of muscarine (10 μM). The increased sIPSCs were largely inhibited by subsequent bath addition of gabazine (1 μM). (B) Cumulative distribution plots showing the effect of muscarine on sIPSC frequency before, after application of muscarine and further addition of gabazine. The distributions of frequency were significantly different among three conditions (control, 0.13 Hz; muscarine, 3.09 Hz; muscarine+gabazine, 0.02 Hz; $P<0.001$ for the control vs. muscarine and $P<0.001$ for muscarine vs. muscarine+gabazine). (C) Cumulative distribution plots showing that muscarine alone did not change the distributions of amplitude, whereas further bath addition of gabazine significantly decreased the distributions of amplitude (muscarine, 27.3±1.0 pA; muscarine+gabazine, 13.8±1.4 pA, $P<0.05$). (D) Bar graph summarizing the effect of muscarine on sIPSC frequency from young GCs (for each input resistance>1 GΩ, on average 1.45±0.1 GΩ, $n=10$). *** $P<0.0005$. (E) Bar graph summarizing the effect of muscarine on sIPSC amplitude from young GCs. (F) Bar graph summarizing the effect of muscarine on sIPSC frequency from mature GCs (for each input resistance<1 GΩ, on average 411±48 MΩ, $n=12$). * $P<0.05$. (G) Bar graph summarizing the effect of muscarine on sIPSC amplitude from mature GCs.

age-clamp configuration. The net current obtained by subtracting the current in the presence of muscarine from the control is quasi-linear and has a reversal potential of −109 mV, very close to the Nernst potential for the K^+-selective channel, suggesting that K^+ channels underlie the background currents. However, further dissection of distinct

types of K^+ channels underlying the relatively small currents (~80 pA at −65 mV) is not possible because of the limited selectivity of available blockers for targeted candidates, such as two-pore-domain K^+ channels and inwardly rectifying K^+ channels. A challenge of future studies will be to use genetic knockout mice to perform precise characterization of specific target channels following mAChR activation.

Despite the fact that the identity of mAChR-coupled K^+ channels remains undetermined here, a single type or a mixture of multiple resting K^+ channels might account for the muscarinic inhibition of resting K^+ currents (McQuiston and Madison, 1999). First, tandem of P domains in a weak inwardly rectifying K^+ channel (TWIK)-1 and TWIK-related K^+-1 channels can give rise to a linear membrane current in physiological solutions (Lesage et al., 1996; Zhou et al., 2009). Second, M_1 receptor activation is known to downmodulate constitutively active two-pore-domain "leak" K^+ channels (Millar et al., 2000) and inwardly rectifying K^+ channels (Carr and Surmeier, 2007). A combination of these two channels might generate a linear *I–V* curve. Finally, other channels such as SK channels and KCNQ/Kv7 subunits associated with KCNE subunits can produce background conductance (Lawrence et al., 2006c). Overall, the muscarine-sensitive K^+ conductance can be generated by variable combinations of these channels or by a yet uncharacterized combination of subunits and auxiliary proteins.

Functional implications

A tonic excitatory drive is required for the generation of gamma oscillations in the interneuron network models (Wang and Buzsáki, 1996; Bartos et al., 2001, 2002, 2007). FS BCs are set in a ready-to-fire mode because of their relatively more depolarized resting potentials than those of principal neurons (Fricker et al., 1999; Verheugen et al., 1999). Therefore, fine tuning of resting membrane potentials by neuromodulators may exert substantial influences on BC activities. During cognitive tasks, cholinergic release increases dramatically (Parikh et al., 2007). The muscarinic excitation of BCs can result in an increase of input resistance and membrane time constant, thereby attenuating the dendritic filtering and augmenting temporal summation of excitatory synaptic potentials in BCs (Geiger et al., 1997; Carr and Surmeier, 2007; Hu et al., 2010). Thus, cholinergic modulation not only depolarizes BCs but also enhances the firing probability and synaptic integration during glutamate transmission. As a consequence, increased cholinergic release can recruit FS BCs to generate emergent gamma-frequency rhythmicity and enhance cortical circuit performance (Fuchs et al., 2007; Sohal et al., 2009). Notably, gamma oscillations often occur as nested rhythm together with theta activity (White et al., 2000; Buzsáki, 2002; Hentschke et al., 2007). In the present study, cholinergic agonists promote the discharge of FS BCs in the theta as well as in the gamma frequency band, an intriguing possibility is that cholinergic activation promotes this nested activity pattern.

Acknowledgments—We thank Dr. C.P. Hung for critically reading the manuscript, Dr. I. Vida for his comments on the manuscript. This work was supported by grants from the Ministry of Education, Taiwan (Aim for The Top University Plan), National Health Research Institutes (NHRI-EX98-9720NC to C.C.L.), Taiwan National Science Council (97-2321-B-010-005 to C.C.L.), Cheng Hsin General Hospital (98-59 to Y.Y.H.) and VGHUST Joint Research Program, Tsou's Foundation (VGHUST97-P6-29 to C.C.L.).

REFERENCES

Aponte Y, Bischofberger J, Jonas P (2008) Efficient Ca^{2+} buffering in fast-spiking basket cells of rat hippocampus. J Physiol 586:2061–2075.

Aponte Y, Lien CC, Reisinger E, Jonas P (2006) Hyperpolarization-activated cation channels in fast-spiking interneurons of rat hippocampus. J Physiol 574:229–243.

Bartos M, Vida I, Frotscher M, Geiger JR, Jonas P (2001) Rapid signaling at inhibitory synapses in a dentate gyrus interneuron network. J Neurosci 21:2687–2698.

Bartos M, Vida I, Frotscher M, Meyer A, Monyer H, Geiger JR, Jonas P (2002) Fast synaptic inhibition promotes synchronized gamma oscillations in hippocampal interneuron networks. Proc Natl Acad Sci U S A 99:13222–13227.

Bartos M, Vida I, Jonas P (2007) Synaptic mechanisms of synchronized gamma oscillations in inhibitory interneuron networks. Nat Rev Neurosci 8:45–56.

Behrends JC, ten Bruggencate G (1993) Cholinergic modulation of synaptic inhibition in the guinea pig hippocampus in vitro: excitation of GABAergic interneurons and inhibition of GABA-release. J Neurophysiol 69:626–629.

Buzsáki G (2002) Theta oscillations in the hippocampus. Neuron 33:325–340.

Carr DB, Surmeier DJ (2007) M_1 mucarinic receptor modulation of Kir2 channels enhances temporal summation of excitatory synaptic potentials in prefrontal cortex pyramidal neurons. J Neurophysiol 97:3432–3438.

Chapman CA, Lacaille JC (1999) Cholinergic induction of theta-frequency oscillations in hippocampal inhibitory interneurons and pacing of pyramidal cell firing. J Neurosci 19:8637–8645.

Cobb SR, Buhl EH, Halasy K, Paulsen O, Somogyi P (1995) Synchronization of neuronal activity in hippocampus by individual GABAergic interneurons. Nature 378:75–78.

Csicsvari J, Jamieson B, Wise KD, Buzsáki G (2003) Mechanisms of gamma oscillations in the hippocampus of the behaving rat. Neuron 37:311–322.

Doischer D, Hosp JA, Yanagawa Y, Obata K, Jonas P, Vida I, Bartos M (2008) Postnatal differentiation of basket cells from slow to fast signaling devices. J Neurosci 28:12956–12968.

Fisahn A, Pike FG, Buhl EH, Paulsen O (1998) Cholinergic induction of network oscillations at 40 Hz in the hippocampus in vitro. Nature 394:186–189.

Fisahn A, Yamada M, Duttaroy A, Gan JW, Deng CX, McBain CJ, Wess J (2002) Muscarinic induction of hippocampal gamma oscillations requires coupling of the M1 receptor to two mixed cation currents. Neuron 33:615–624.

Freund TF, Katona I (2007) Perisomatic inhibition. Neuron 56:33–42.

Fricker D, Verheugen JA, Miles R (1999) Cell-attached measurements of the firing threshold of rat hippocampal neurones. J Physiol 517:791–804.

Fries P, Reynolds JH, Rorie AE, Desimone R (2001) Modulation of oscillatory neuronal synchronization by selective visual attention. Science 291:1560–1563.

Frotscher M, Léránth C (1985) Cholinergic innervation of the rat hippocampus as revealed by choline acetyltransferase immunocytochemistry: a combined light and electron microscopic study. J Comp Neurol 239:237–246.

Fuchs EC, Zivkovic AR, Cunningham MO, Middleton S, Lebeau FE, Bannerman DM, Rozov A, Whittington MA, Traub RD, Rawlins JN, Monyer H (2007) Recruitment of parvalbumin-positive interneurons determines hippocampal function and associated behavior. Neuron 53:591–604.

Geiger JR, Lübke J, Roth A, Frotscher M, Jonas P (1997) Submillisecond AMPA receptor-mediated signaling at a principal neuron-interneuron synapse. Neuron 18:1009–1023.

Gorelova N, Seamans JK, Yang CR (2002) Mechanisms of dopamine activation of fast-spiking interneurons that exert inhibition in rat prefrontal cortex. J Neurophysiol 88:3150–3166.

Gray CM, Singer W (1989) Stimulus-specific neuronal oscillations in orientation columns of cat visual cortex. Proc Natl Acad Sci U S A 86:1698–1702.

Gulledge AT, Park SB, Kawaguchi Y, Stuart GJ (2007) Heterogeneity of phasic cholinergic signaling in neocortical neurons. J Neurophysiol 97:2215–2229.

Hájos N, Pálhalmi J, Mann EO, Németh B, Paulsen O, Freund TF (2004) Spike timing of distinct types of GABAergic interneuron during hippocampal gamma oscillations in vitro. J Neurosci 24: 9127–9137.

Hájos N, Papp EC, Acsády L, Levey AI, Freund TF (1998) Distinct interneuron types express m2 muscarinic receptor immunoreactivity on their dendrites or axon terminals in the hippocampus. Neuroscience 82:355–376.

Hefft S, Kraushaar U, Geiger JR, Jonas P (2002) Presynaptic short-term depression is maintained during regulation of transmitter release at a GABAergic synapse in rat hippocampus. J Physiol 539:201–208.

Hentschke H, Perkins MG, Pearce RA, Banks MI (2007) Muscarinic blockade weakens interaction of gamma with theta rhythms in mouse hippocampus. Eur J Neurosci 26:1642–1656.

Hille B (2001) Ion channels of excitable membranes, 3rd ed. Sunderland, MA: Sinauer.

Hu H, Martina M, Jonas P (2010) Dendritic mechanisms underlying rapid synaptic activation of fast-spiking hippocampal interneurons. Science 327:52–58.

Kawaguchi Y (1997) Selective cholinergic modulation of cortical GABAergic cell subtypes. J Neurophysiol 78:1743–1747.

Klausberger T, Somogyi P (2008) Neuronal diversity and temporal dynamics: the unity of hippocampal circuit operations. Science 321:53–57.

Kole MH, Stuart GJ (2008) Is action potential threshold lowest in the axon? Nat Neurosci 11:1253–1255.

Kruglikov I, Rudy B (2008) Perisomatic GABA release and thalamocortical integration onto neocortical excitatory cells are regulated by neuromodulators. Neuron 58:911–924.

Lamour Y, Dutar P, Jobert A (1982) Excitatory effect of acetylcholine on different types of neurons in the first somatosensory neocortex of the rat: laminar distribution and pharmacological characteristics. Neuroscience 7:1483–1494.

Lawrence JJ, Grinspan ZM, Statland JM, McBain CJ (2006a) Muscarinic receptor activation tunes mouse stratum oriens interneurones to amplify spike reliability. J Physiol 571:555–562.

Lawrence JJ, Saraga F, Churchill JF, Statland JM, Travis KE, Skinner FK, McBain CJ (2006c) Somatodendritic Kv7/KCNQ/M channels control interspike interval in hippocampal interneurons. J Neurosci 26:12325–12338.

Lawrence JJ, Statland JM, Grinspan ZM, McBain CJ (2006b) Cell type-specific dependence of muscarinic signalling in mouse hippocampal stratum oriens interneurones. J Physiol 570:595–610.

Lawrence JJ (2008) Cholinergic control of GABA release: emerging parallels between neocortex and hippocampus. Trends Neurosci 31:317–327.

Lee MG, Chrobak JJ, Sik A, Wiley RG, Buzsáki G (1994) Hippocampal theta activity following selective lesion of the septal cholinergic system. Neuroscience 62:1033–1047.

Léránth C, Frotscher M (1987) Cholinergic innervation of hippocampal GAD- and somatostatin-immunoreactive commissural neurons. J Comp Neurol 261:33–47.

Lesage F, Guillemare E, Fink M, Duprat F, Lazdunski M, Romey G, Barhanin J (1996) TWIK-1, a ubiquitous human weakly inward rectifying K^+ channel with a novel structure. EMBO J 15:1004–1011.

Lien CC, Jonas P (2003) Kv3 potassium conductance is necessary and kinetically optimized for high-frequency action potential generation in hippocampal interneurons. J Neurosci 23:2058–2068.

Lien CC, Martina M, Schultz JH, Ehmke H, Jonas P (2002) Gating, modulation and subunit composition of voltage-gated K^+ channels in dendritic inhibitory interneurones of rat hippocampus. J Physiol 538:405–419.

Lisman J, Buzsáki G (2008) A neural coding scheme formed by the combined function of gamma and theta oscillations. Schizophr Bull 34:974–980.

Lucas-Meunier E, Fossier P, Baux G, Amar M (2003) Cholinergic modulation of the cortical neuronal network. Pflugers Arch 446: 17–29.

Mann EO, Suckling JM, Hájos N, Greenfield SA, Paulsen O (2005) Perisomatic feedback inhibition underlies cholinergically induced fast network oscillations in the rat hippocampus in vitro. Neuron 45:105–117.

Mathie A (2007) Neuronal two-pore-domain potassium channels and their regulation by G protein-coupled receptors. J Physiol 578: 377–385.

McQuiston AR, Madison DV (1999) Muscarinic receptor activity has multiple effects on the resting membrane potentials of CA1 hippocampal interneurons. J Neurosci 19:5693–5702.

Millar JA, Barratt L, Southan AP, Page KM, Fyffe RE, Robertson B, Mathie A (2000) A functional role for the two-pore domain potassium channel TASK-1 in cerebellar granule neurons. Proc Natl Acad Sci U S A 97:3614–3618.

Ming GL, Song H (2005) Adult neurogenesis in the mammalian central nervous system. Annu Rev Neurosci 28:223–250.

Nicoll RA (1988) The coupling of neurotransmitter receptors to ion channels in the brain. Science 241:545–551.

Nishikawa M, Munakata M, Akaike N (1994) Muscarinic acetylcholine response in pyramidal neurones of rat cerebral cortex. Br J Pharmacol 112:1160–1166.

Parikh V, Kozak R, Martinez V, Sarter M (2007) Prefrontal acetylcholine release controls cue detection on multiple timescales. Neuron 56:141–154.

Parra P, Gulyás AI, Miles R (1998) How many subtypes of inhibitory cells in the hippocampus? Neuron 20:983–993.

Porter JT, Cauli B, Tsuzuki K, Lambolez B, Rossier J, Audinat E (1999) Selective excitation of subtypes of neocortical interneurons by nicotinic receptors. J Neurosci 19:5228–5235.

Scuvée-Moreau J, Seutin V, Dresse A (1998) A quantitative pharmacological study of the cholinergic depolarization of hippocampal pyramidal cells in rat brain slices. Arch Physiol Biochem 105: 365–372.

Sohal VS, Zhang F, Yizhar O, Deisseroth K (2009) Parvalbumin neurons and gamma rhythms enhance cortical circuit performance. Nature 459:698–702.

Stocca G, Schmidt-Hieber C, Bischofberger J (2008) Differential dendritic Ca^{2+} signalling in young and mature hippocampal granule cells. J Physiol 586:3795–3811.

Talley EM, Lei Q, Sirois JE, Bayliss DA (2000) TASK-1, a two-pore domain K^+ channel, is modulated by multiple neurotransmitters in motoneurons. Neuron 25:399–410.

Verheugen JA, Fricker D, Miles R (1999) Noninvasive measurements of the membrane potential and GABAergic action in hippocampal interneurons. J Neurosci 19:2546–2555.

Volpicelli LA, Levey AI (2004) Muscarinic acetylcholine receptor subtypes in cerebral cortex and hippocampus. Prog Brain Res 145:59–66.

Wang XJ, Buzsáki G (1996) Gamma oscillation by synaptic inhibition in a hippocampal interneuronal network model. J Neurosci 16:6402–6413.

Watkins CS, Mathie A (1996) A non-inactivating K^+ current sensitive to muscarinic receptor activation in rat cultured cerebellar granule neurons. J Physiol 491:401–412.

White JA, Banks MI, Pearce RA, Kopell NJ (2000) Networks of interneurons with fast and slow gamma-aminobutyric acid type A ($GABA_A$) kinetics provide substrate for mixed gamma-theta rhythm. Proc Natl Acad Sci U S A 97:8128–8133.

Xiang Z, Huguenard JR, Prince DA (1998) Cholinergic switching within neocortical inhibitory networks. Science 281:985–988.

Zhou M, Xu G, Xie M, Zhang X, Schools GP, Ma L, Kimelberg HK, Chen H (2009) TWIK-1 and TREK-1 are potassium channels contributing significantly to astrocyte passive conductance in rat hippocampal slices. J Neurosci 29:8551–8564.

(Accepted 22 April 2010)
(Available online 28 April 2010)